Materials Research Proceedings **17** (2020) 138-145 https://doi.org/10.21741/9781644901038-21

Influence of Electrode Material on Surface Roughness during Die-Sinking Electrical Discharge Machining of Inconel 718

CHWALCZUK Tadeusz[1,a], FELUSIAK Agata[1,b*], WICIAK-PIKUŁA Martyna[1,c] and KIERUJ Piotr[1,d]

[1] Poznań University of Technology, Piotrowo 3 St., 60-965 Poznan, Poland

[a] tadeusz.chwalczuk@put.poznan.pl, [b*]agata.z.felusiak@doctorate.put.poznan.pl, [c] martyna.r.wiciak@doctorate.put.poznan.pl, [d] piotr.kieruj@put.poznan.pl

Keywords: Die-Sinking Electric Discharge Machining, EDM, Surface Roughness, Inconel 718, Electrode Materials

Abstract. The article presents an analysis of the impact of electrode material and its roughness on the surface roughness of a machined surface. An Inconel 718 element was machined with four different electrodes with constant machining parameters. It was proved that under certain conditions there is a relationship between the roughness of an electrode and a machined surface. The research results show that considering the quality of a machined surface, the copper alloy electrode gives the highest predictability of roughness parameters.

Introduction

Nickel-based alloys are difficult to machine with traditional methods such as turning or milling [1]. Difficulty in machining, among others, is connected with the creation of adhesive bonds with the tool material, which results in build-ups, low thermal conductivity compared to carbon steel and tendency to strengthen during machining [2,3]. With traditional machining of such materials, it is difficult to ensure adequate surface roughness [4]. Ensuring adequate roughness and properties of manufactured parts is extremely important from the point of view of performance [5,6].

Due to the difficulties which occur during machining with traction methods, unconventional methods such as laser assisted machining are being increasingly used (LAM) [7]. In [8], the authors used different laser powers to study the effect on stainless steel microstructure. The use of a laser, however, involves the possibility of changing the properties of the surface layer [9]. The use of electrical discharge machining (EDM) is another method. It involves removing material due to controlled electrical discharges which occur between the electrode (tool) and the workpiece. The method is used for the production of machine parts such as noncircular cogbelt pulleys [10]. However, this is not a high-performance manufacturing method [11, 12]. The authors [13] point out that the right choice of an electrode is important in the EDM process. In their research, the machining stainless steel used three electrode materials: aluminum, copper and graphite, at different levels of current. According to their research, the best result (proportion of removed material to electrode wear) was obtained for the current of 6.5 [A] for a graphite electrode. In [14], the authors examined two electrode materials, brass and tungsten carbide, when machining stainless steel and tungsten carbide, with variable process parameters. As a result of the research, they noticed that the brass electrode wears more than the WC electrode, however, it also removes the workpiece faster, due to higher electrical conductivity. In [15], the authors studied electrodes made of aluminum, stainless steel, brass, copper and graphite. Researchers have found that graphite has the best properties as an electrode material. This electrode ensures the fastest material removal and has the lowest wear due to the highest melting

point among the mentioned materials. In [16], the authors compared two electrode materials, namely brass and tungsten carbide, when machining aluminum, stainless steel and tungsten carbide. It was noticed that the electrode material has an effect on roughness. With low discharge energy, when machining stainless steel using tungsten carbide, the electrode obtained about 2.5 times lower parameter value *Ra* (0,23 μm) than with the brass electrode (0,57 μm), while with the increase of the discharge energy, the value of the roughness parameter *Ra* for the tungsten carbide electrode increased rapidly (1,1 μm) and was almost twice as high as for the brass electrode (0,67 μm). In [17], the authors considered three types of electrodes, such as copper, brass and graphite. They studied the material removal rate (MRR) and surface roughness and found that the material removal rate was higher for the copper electrode than for the brass one. The surface finishing was better for brass than for the copper electrode, and MRR and roughness parameters obtained using a graphite electrode were average. Electrodes and machine parts should be manufactured from a high-quality semi-product, without the separation of alloyed elements and devoid of shrinkage. This is ensured by the use of numerical methods [18].

The obtained results may be interesting for other industries that use EDM or use similar methods, e.g. heavy working machines [19, 20] or applying protective coatings by electro-spark deposition [21, 22]. The effects can also be inspiring for image analysis methods [23] and for health and safety issues [24].

Experimental details

The tests were carried out on a sample made of Inconel 718 using an Agie Charmilles Cabinet SP1U spark machining machine. A synthetic hydrocarbon fluid EDM fluid 108 MP-SE was used during machining. The tests were carried out with constant parameters shown in Table 1. Four electrodes made of different materials, the following were used in the experiment: copper impregnated graphite, copper alloy, small grain graphite (grain size <5 μm), large grain graphite (grain size 14 μm). Table 2 presents the percentage of chemical composition of the electrode materials.

Table 1. Experimental settings.

parametr	*Peak current* [A]	*spark gap* [mm]	*Electrode polarity*	*cutting depth* [mm]
value	10	0.2	+	0.5

Table 2. Percentage chemical composition of electrode materials

Component	Copper impregnated graphite	Copper alloy	Large grain graphite	Small grain graphite
Si	0.08	0.62	0.10	0.14
Cr	1.22	12.99	3.01	3.38
Fe	3.12	39.44	7.08	8.58
Ni	0.33	3.66	0.99	0.97
Cu	6.26	42.62	0.00	0.00
S	0.20	0.67	0.35	0.37
C	88.79	0.00	88.46	86.56

Materials Research Proceedings **17** (2020) 138-145 https://doi.org/10.21741/9781644901038-21

Copper impregnated graphite formation based on technologies of the liquid matrix consists in infiltrating a porous structure of the composite reinforcement phase with a liquid technical alloy [25, 26]. Four operations were performed with each electrode. After each operation, the roughness of treated surface and electrode surface were measured. Roughness parameters were estimated from the area dimensions of 1,5x1,5mm. For the surface topography assessment, stationary profilographometer T8000 was carried out. The following roughness parameters were measured: the texture direction *St*, arithmetic mean height of surface *Sa*, the maximum value peak height on surface *Sp*, the maximum value valley depth *Sv*, the maximum height of surface *Sz*, the root mean squared height *Sq, the* kurtosis of 3D surface texture *Sku*, Skewness *Ssk*.

Results analysis

Figure 1 shows the electrodes after four passes. On the basis of the obtained results, the change in electrode roughness and workpiece rosughness over time (Fig.2) and the correlation between electrode roughness and values of workpiece surface roughness parameters were analyzed (Fig. 3).

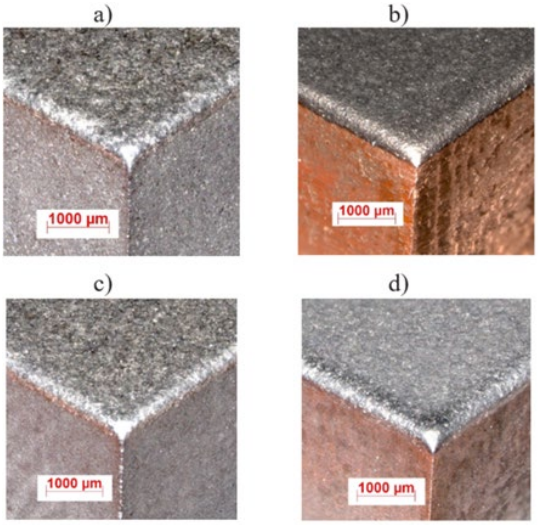

Fig.1. Electrodes after a completed series of tests: a) large grain graphite, b) copper alloy, c) small grain graphite, d) copper impregnated graphite

The next picture (Fig.4) shows the topography of the surface worked after the last pass. The graphs in Figure 4 show the relationships between some parameters of the machining surface roughness and the working surface of the electrodes: the texture direction *St,* arithmetic mean height of surface *Sa,* the maximum height of surface *Sz,* the kurtosis of 3D surface texture *Sku.*

Analyzing the graphs of *Sa,* the parameters change (Fig.2a and Fig.2b) over time for the electrodes and workpiece. A satisfactory correlation can be seen only for the copper impregnated graphite electrode. Very high correlation occurs for the surface treated with the Large grain graphite electrode, but the *Sa* values themselves have a large spread. The opposite situation can be observed for the electrolytic copper electrode. For small grain graphite, no correlation can be found over time.

Analyzing the *Sz/St* graph (Fig.2c), it can be stated that the surface is equalized for the copper alloy electrode and the tips are worn during machining. In the case of other electrodes, the tendency is reversed as there are more vertices and / or valleys, and the dispersion of results is large, which may indicate a random removal of graphite grains from the electrodes. The analysis of the skewness of the electrode roughness profile (Fig.2d) indicates the increase in the

Materials Research Proceedings **17** (2020) 138-145 https://doi.org/10.21741/9781644901038-21

proportion of vertices in the electrodes containing graphite over time, while in the case of copper electrodes they are sheared.

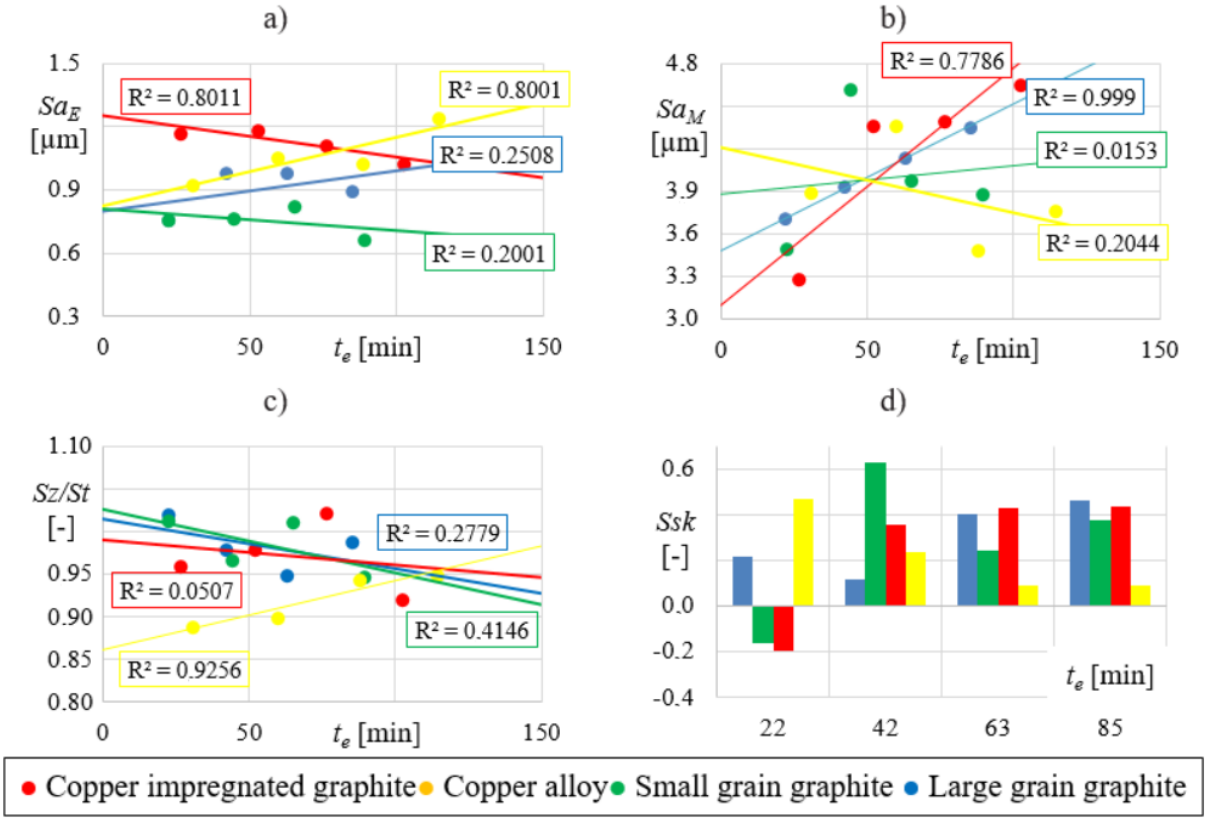

Fig.2. Course of roughness parameters in time a) Sa of the electrode surface, b) Sa of the treated surface, c) ratio of Sz to St of the electrode surface, d) Ssk of the electrode surface

It can be seen in the above graphs that the correlation between the roughness of the electrode working surface and the machining surface roughness is ambiguous and does not occur in a satisfactory correlation for some electrode materials.

In the case of graphite electrodes, grain size has a significant impact on this relation. For the large grain graphite, the correlation is very high, usually above 0.9. However, with some parameters for the small grain graphite, there is no relation between the roughness of the treated surface and the electrode. In the case of the *Sa* parameter (Fig. 3d), no relationship can be demonstrated for the copper alloy and the small grain graphite electrodes.

Analyzing these graphs and Table 3, it can be seen that the roughness of electrode surface affects the directivity of the treated surface and kurtosis regardless of the electrode material used. In the case of height parameters, the correlation occurs for the large grain graphite electrode and copper impregnated graphite electrode. For amplitude parameters, the best correlation is for copper and the copper impregnated graphite electrode. It should be noted that the high correlation of valleys on the electrode surface with the peaks on the treated surface occurs (Fig.3b). The inverse relation does not occur (Table 3), which suggests that the peaks on the working surface of the electrode wear during discharge.

Materials Research Proceedings **17** (2020) 138-145 https://doi.org/10.21741/9781644901038-21

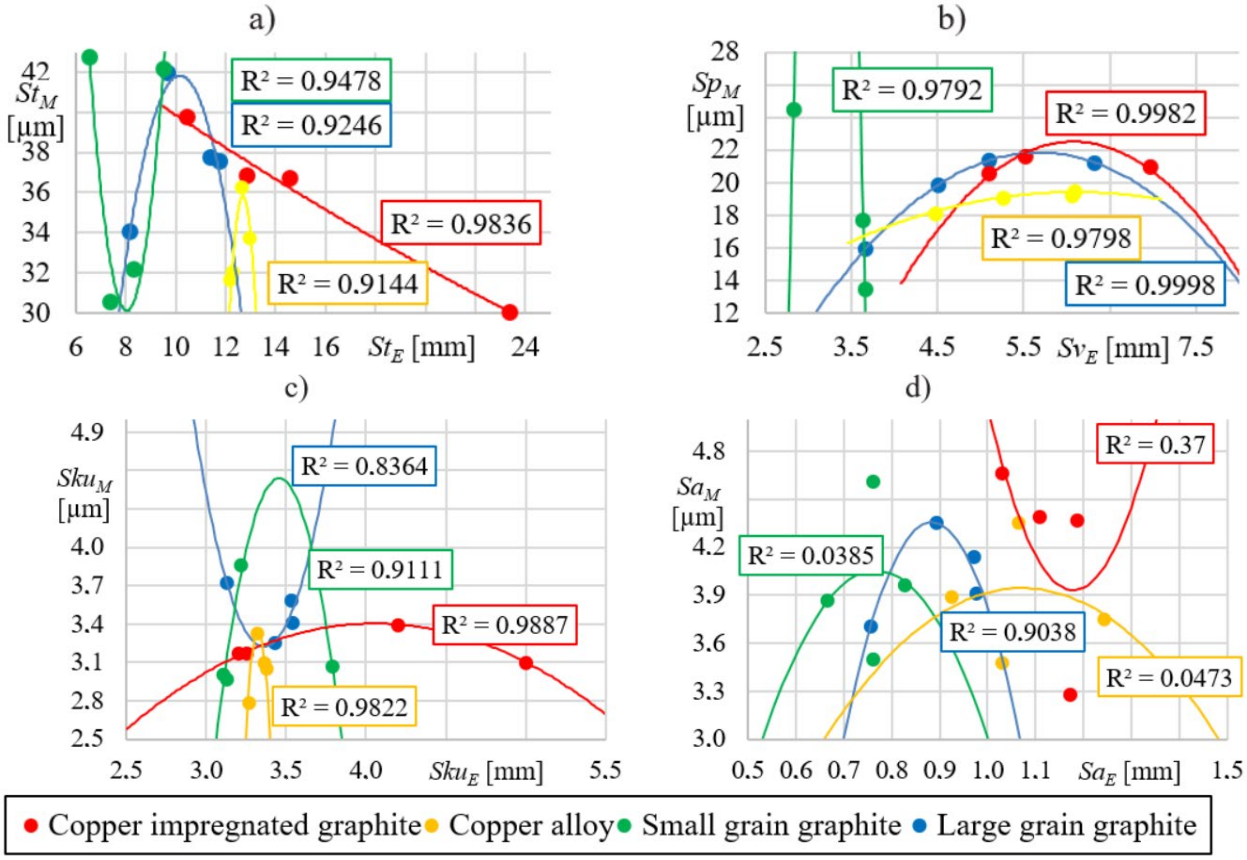

Fig.3. Correlation between the roughness parameters of machined surface and electrode roughness a) St, b) Sa, c) Sz, d) Sku

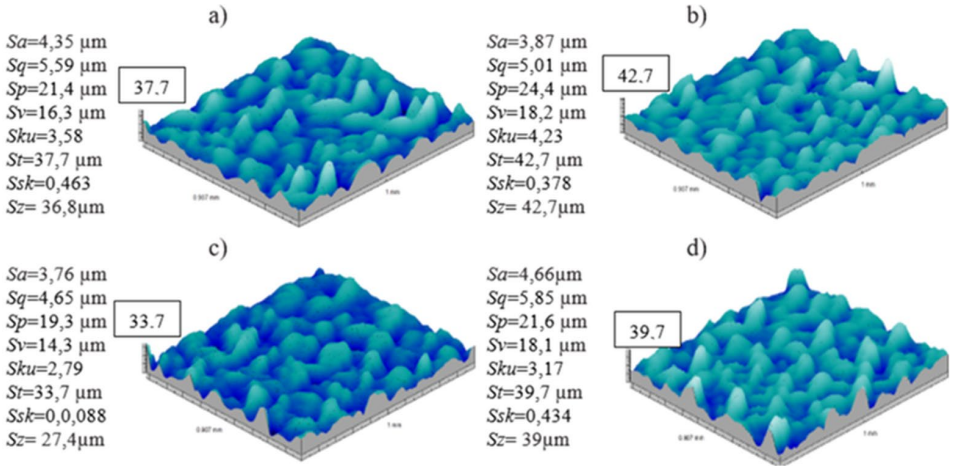

Fig. 4. Topography of the worked surface for the electrode: a) large grain graphite, b) small grain graphite, c) copper alloy, d) copper impregnated graphite.

Table 3. Polynomial regression equations and correlation coefficient values for individual electrodes

parametr		LGG	SGG	CIG	EA
Sq_M / Sq_E	eql.	-34.343 Sq_E^2 + 77.13 Sq_E – 37.735	-10.09 Sq_E^2 + 19.192 Sq_E – 3.9968	-12.314Sq_E^2+ 32.326Sq_E-15.385	-3.6128Sq_E^2 + 9.3599Sq_E-1.1131
	R^2	0,84	0,011	0.98	0.07
Sv_M / Sp_E	eql.	-2.7775 Sp_E^2+ 33.208 Sp_E- 77.579	-5.9657 Sp_E^2 + 57.001 Sp_E – 111.05	0.1044 Sp_E^2- 1.8771Sp_E+24.631	= 1.7945Sp_E^2- 23.108Sp_E +89.22
	R^2	0.99	0.34	0.29	0.15
Ssk_M / Ssk_E	eql.	-9.8908Ssk_E^2+ 0.915Ssk_E+ 0.4213	= -30.641Ssk_E^2 + 8.566Ssk_E + 0.2357	-15.462Ssk_E^2+ 2.723Ssk_E+0.8418	= 5.012Ssk_E^2+ 0.810Ssk_E+0.115
	R^2	0.31	0,67	0.92	0.99
Sz_M / Sz_E	eql.	-1.5604 Sz_E^2 + 30.967 Sz_E – 116.35	= 0.929 Sz_E^2 – 16.857 Sz_E + 108.81	-0.0204Sz_E^2- 0.167 Sz_E+ 42.049	-2.2886Sz_E^2+ 46.606Sz_E- 204.83
	R^2	0.98	0.41	0.97	0.41

As can be seen in Fig.3, only for machining using the copper alloy electrode, roughness parameters *Sa* have a lower value after the last pass than after the first pass. The surface quality after the treatment with small grain graphite electrode is difficult to predict. Due to the high correlation of results, the prediction of the surface roughness treated with the copper impregnated graphite and large grain graphite electrode is the easiest. For some parameters it is also possible to predict the results for the other two electrodes.

Conclusions

On the basis of conducted research, the following conclusions were formulated:

- Due to the quality of a machined surface, it is most reasonable to use copper alloy electrodes. The use of this electrode allowed for obtaining the lowest values of *Sa* parameters in the last pass.
- There is a correlation between the roughness of a machined surface and the roughness of an electrode, but it is not a linear relation. Its shape depends on the electrode material. This relation does not exist for all tested electrode materials. This should be noted when choosing the electrode.
- For graphite electrodes, the size of graphite grains is significant. The roughness of a surface machined with the large grain graphite electrode depends on the roughness of the electrode itself. The increase of roughness parameters in subsequent passes is stable. With the small grain graphite electrode, the correlation between the roughness of the electrode and the machined surface is less often obtained, it is also more difficult to predict the roughness in subsequent passes.

References

[1] M. Kukliński, A. Bartkowska, D. Przestacki, Investigation of laser heat treated Monel 400, MATEC Web of Conferences 219 (2018) 02005-1-8. https://doi.org/10.1051/matecconf/201821902005

[2] A. Bartkowska, A. Pertek, M. Popławski, D. Przestacki, A. Miklaszewski, Effect of laser modification of B-Ni complex layer on wear resistance and microhardness, Optics and Laser Technology 72 (2015) 116-124. https://doi.org/10.1016/j.optlastec.2015.03.024

[3] P. Kieruj, N. Makuch, M. Kukliński, Characterization of laser-borided Nimonic 80A-alloy, MATEC Web of Conferences 188 (2018) 02003-1-8. https://doi.org/10.1051/matecconf/201818802003

[4] D. Przestacki, R. Majchrowski, L. Marciniak-Podsadna, Experimental research of surface roughness and surface texture after laser cladding, App. Surf. Sci. 388 (2016) 420-423. https://doi.org/10.1016/j.apsusc.2015.12.093

[5] Z. Ignaszak, P. Popielarski, J. Hajkowski, E. Codina, Methodology of comparative validation of selected foundry simulation codes, Arch. Foundry Eng. 15 (2015) 37-44. https://doi.org/10.1515/afe-2015-0076

[6] P. Twardowski, M. Tabaszewski, S. Wojciechowski, Turning process monitoring of internal combustion engine piston's cylindrical surface, MATEC Web of Conferences 112 (2017) 10002-1-6. https://doi.org/10.1051/matecconf/201711210002

[7] M. Kawalec, D. Przestacki, K. Bartkowiak, M. Jankowiak, Laser assisted machining of aluminum composite reinforced by SiC particle, ICALEO Congress Proc. (2008) 895-900. https://doi.org/10.2351/1.5061278

[8] D. Przestacki, A. Bartkowska, M. Kukliński, P. Kieruj, The effects of laser surface modification on microstructure of 1.4550 Stainless steel, MATEC Web of Conferences 237 (2018) 02009-1-5. https://doi.org/10.1051/matecconf/201823702009

[9] J. Hajkowski, P. Popielarski, Z. Ignaszak, Cellular Automaton Finite Element Method Applied for Microstructure Prediction of Aluminum Casting Treated by Laser Beam, Arch. Foundry Eng. 19 (2019) 111-118.

[10] P. Krawiec, M. Grzelka, J. Kroczak, G. Domek, A. Kołodziej, A proposal of measurement methodology and assessment of manufacturing methods of nontypical cog belt pulleys, Measurement 132 (2019) 182-190. https://doi.org/10.1016/j.measurement.2018.09.039

[11] M. Kujawski, P.Krawiec, Analysis of Generation Capabilities of Noncircular Cog belt Pulleys on the Example of a Gear with an Elliptical Pitch Line, Journal of Manufacturing Science and Engineering-Transactions of the ASME 133 (5) (2011) 051006-1-7. https://doi.org/10.1115/1.4004866

[12] P. Krawiec, A. Marlewski, Spline description of not typical gears for belt transmissions, Journal of Theoretical and Applied Mechanics 49 (2) (2011) 355-367.

[13] M.H.F. Al Hazza, A.A. Khan, M.Y. Ali, S.F. Hasim, M.R.C. Daud, A study on capabilities of different electrode materials during electrical discharge machining (EDM), IIUM Engineering Journal 18 (2) (2017) 189-195. https://doi.org/10.31436/iiumej.v18i2.755

[14] G. D'Urso, G. Maccarini, C. Ravasio, Influence of electrode material in micro-EDM drilling of stainless steel and tungsten carbide, International Journal of Advanced Manufacturing Technology 85 (2016) 2013-2025. https://doi.org/10.1007/s00170-015-7010-9

[15] G. Zhu, Q. Zhang, K. Wang, Y. Huang, J. Zhang, Effects of Different Electrode Materials on High-speed Electrical Discharge Machining of W9Mo3Cr4V, Procedia CIRP 68 (2018) 64-69. https://doi.org/10.1016/j.procir.2017.12.023

[16] G. D'Urso, C. Ravasio, Material-Technology Index to evaluate micro-EDM drilling process, Journal of Manufacturing Processes 26 (2017) 13-21. https://doi.org/10.1016/j.jmapro.2017.01.003

[17] S. Choudhary, K. Kant, P. Saini, Analysis of MRR and SR with Different Electrode for SS 316 on Die-Sinking EDM using Taguchi Technique, Global Journal of Researches in Engineering Mechanical and Mechanics Engineering 13 (2013) 14-21.

[18] P.Krawiec, K.Waluś, Ł.Warguła, J.Adamiec, Wear evaluation of elements of V-belt transmission with the application of optical microscope, MATEC Web of Conferences 157 (2018), 01009-1-8. https://doi.org/10.1051/matecconf/201815701009

[19] M. Domagala, H. Momeni, J. Domagala-Fabis, G. Filo, D. Kwiatkowski, Simulation of cavitation erosion in a hydraulic valve. Materials Research Proceedings 5 (2018) 1-6. https://doi.org/10.21741/9781945291814-1

[20] A. Pacana, K. Czerwinska, R. Dwornicka, Analysis of non-compliance for the cast of the industrial robot basis, METAL 2019 28th Int. Conf. on Metallurgy and Materials (2019), Ostrava, Tanger 644-650. https://doi.org/10.37904/metal.2019.869

[21] R. Dwornicka, N. Radek, M. Krawczyk, P. Osocha, J. Pobedza, The laser textured surfaces of the silicon carbide analyzed with the bootstrapped tribology model. METAL 2017 26th Int. Conf. on Metallurgy and Materials (2017), Ostrava, Tanger 1252-1257.

[22] N. Radek, A. Szczotok, A. Gadek-Moszczak, R. Dwornicka, J. Broncek, J. Pietraszek, The impact of laser processing parameters on the properties of electro-spark deposited coatings. Arch. Metall. Mater. 63 (2018) 809-816.

[23] A. Gadek-Moszczak, J. Pietaszek, B. Jasiewicz, S. Sikorska, L. Wojnar, The Bootstrap Approach to the Comparison of Two Methods Applied to the Evaluation of the Growth Index in the Analysis of the Digital X-ray Image of a Bone Regenerate. New Trends in Comp. Collective Intell. 572 (2015) 127-136. https://doi.org/10.1007/978-3-319-10774-5_12

[24] L. Chybowski, K. Gawdzinska, O. Slesicki, K. Patejuk, G. Nowosad, An engine room simulator as an educational tool for marine engineers relating to explosion and fire prevention of marine diesel engines. Scientific Journals of the Maritime University of Szczecin 43 (2015) 15-21.

[25] K. Gawdzińska, L. Chybowski, A. Bejger, S. Krile, Determination of technological parameters of saturated composites based on sic by means of a model liquid, Metalurgija 55(4) (2016) 659-662.

[26] K. Gawdzińska, L. Chybowski, W. Przetakiewicz, R. Laskowski, Application of FMEA in the Quality Estimation of Metal Matrix Composite Castings Produced by Squeeze Infiltration, Arch. Metall. Mater. 62 (4) (2017) 2171-2182. https://doi.org/10.1515/amm-2017-0320